Oxidation of CO on Gold-Covered Pt(335)

D. C. Skelton,[†,§] R. G. Tobin,[†,‡] David K. Lambert,*[,†,§] Craig L. DiMaggio,[§] and Galen B. Fisher[†,§]

Center for Sensor Materials, Michigan State University, East Lansing, Michigan 48824-1116, Department of Physics and Astronomy, Tufts University, Medford, Massachusetts 02155, and General Motors Research and Development Center, Warren, Michigan 48090-9055

Received: September 10, 1998; In Final Form: November 30, 1998

We have studied the adsorption and reaction of oxygen and CO on a stepped Pt surface with varying amounts of Au, using temperature-programmed desorption and reaction (TPD and TPR), low-energy electron diffraction (LEED), high-resolution electron energy loss spectroscopy, and steady-state reaction measurements. When the surface is fully covered with Au it is inert to oxygen adsorption and to CO oxidation, and supports only a single weakly bound CO adsorption state. The surface covered with 0.7 ML Au, however, exhibits properties different from either bare Pt or bare Au. Our TPD and LEED results suggest the coexistence of completely Au-covered regions and regions with Au on the step edges but not on the terraces. Dissociative oxygen adsorption is reduced by 90%, and the remaining oxygen is confined to Pt sites near the Au/Pt boundaries. The Au-covered regions support weakly bound CO adsorption states with desorption temperatures of 120, 190, and 240 K. CO in these states can diffuse rapidly and react efficiently with adsorbed atomic oxygen at temperatures as low as 150 K. In low-temperature TPR experiments the reaction is limited by the availability of adsorbed oxygen under almost all conditions. Under steady-state conditions, however, it is limited by the availability of CO even at low temperatures and CO partial pressures up to 10^{-6} Torr. Adding CO partial pressure does not inhibit the reaction. Consequently, adsorbed CO does not completely block all the sites at which oxygen dissociates on this surface, unlike on bare platinum.

1. Introduction

Exhaust oxygen sensors with platinum electrodes are a mature automotive technology. Adding gold to the electrode material has been shown[1,2] to increase the sensor's sensitivity to oxidizable gases such as CO, H_2, and hydrocarbons. The modified sensors might eventually be used for on-board detection of catalytic converter malfunction. However, there is little understanding of how they work. With platinum electrodes, the electrode exposed to exhaust gas has sufficient catalytic activity to drive the CO-oxidation reaction to equilibrium. One proposed explanation of how adding gold affects the sensor's response is that it simply decreases the electrode's catalytic activity. To increase our understanding of the sensing mechanism, we have studied the effect that adding gold has on CO oxidation at a stepped Pt surface.

The oxidation of CO on Pt has been extensively studied.[3−23] Under most conditions the primary mechanism is a Langmuir−Hinshelwood (LH) reaction between mobile adsorbed CO and immobile adsorbed atomic oxygen. On Pt(111) it occurs primarily near 320 K, with product CO_2 leaving the surface immediately. The reaction is considered structure-insensitive[3,24] even though there have been reports that the reaction rate depends on a supported Pt catalyst's particle size.[22,23] Since preadsorbed CO poisons the surface for subsequent oxygen adsorption, while preadsorbed oxygen does not prevent CO adsorption, the CO_2 yield is frequently determined by the oxygen coverage.[3,10] Energetic O atoms can react with CO at temperatures below 150 K. This has been seen with "hot" O atoms obtained from the thermal[8] or photon-induced[14,15] dissociation of adsorbed O_2, or from an atomic beam.[13] A small yield has also been reported near 230 K between adsorbed CO and disordered adsorbed atomic oxygen.[11]

On stepped Pt surfaces, Yates and co-workers have shown that CO at terrace sites is most reactive.[16−19] Consequently, the CO reaction probability decreases with increasing step density.[20] Oxygen dissociation, however, occurs primarily at step or defect sites,[25−27] causing oxygen's sticking probability to increase exponentially with step density.[20] In addition, oxygen and CO compete for step and terrace sites. The overall reaction kinetics are complex.[21] Our results indicate that a submonolayer coverage of gold on Pt(335) significantly reduces the capacity of the surface to adsorb oxygen, but at the same time it opens a new low-temperature oxidation pathway for CO.

O_2 does not dissociate thermally on gold. As a result, gold does not ordinarily catalyze CO oxidation. Oxidation occurs below 300 K if the gold surface is exposed to gas-phase atomic O or to a molecule, such as O_3, with weakly bound oxygen.[28−30] If atomic O is provided, CO does oxidize on gold at relatively low temperatures.[31−36] It occurs at temperatures as low as 200 K on gold particles on a metal oxide−an O source.[31]

Our substrate was Pt(335) or Pt(s)[4(111)×(100)] in step-terrace notation. It has four-atom-wide (111) terraces separated by monatomic (100) steps. We find that when Pt(335) is dosed with more than one monolayer of gold (1 ML = one adsorbate per surface Pt atom), it is unable to dissociate O_2 and is inert for CO oxidation. On a *partially* Au-covered Pt(335) crystal, however, the gold blocks many of the step sites and suppresses,

* Author to whom correspondence should be addressed.
† Center for Sensor Materials, Michigan State University.
‡ Department of Physics and Astronomy, Tufts University.
§ General Motors Research and Development Center.

10.1021/jp983670o CCC: $18.00
Published on Web 01/22/1999

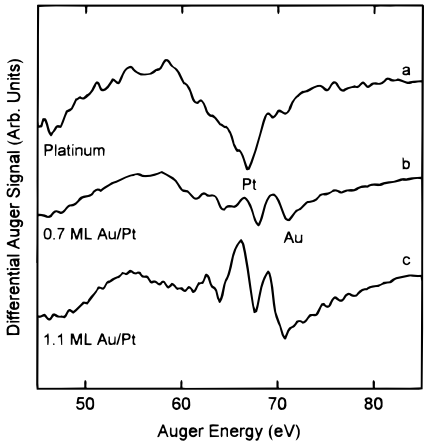

Figure 1. Auger signal at three coverages of gold on Pt(335): (a) bare Pt(335), (b) 0.7 ML Au/Pt(335), and (c) 1.1 ML Au/Pt(335). The relative intensities of the Au and Pt peaks can be related to gold coverage.

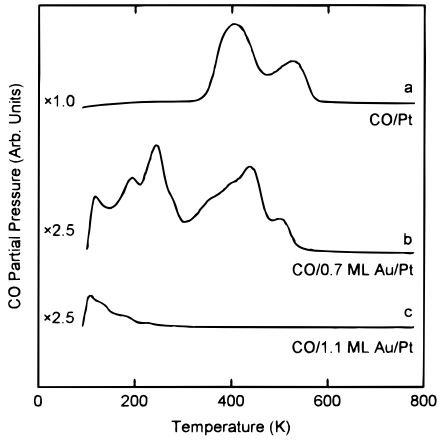

Figure 2. Desorption of a saturation coverage of CO with three gold coverages: (a) gold free Pt(335), (b) 0.7 ML Au/Pt(335), and (c) 1.1 ML Au/Pt(335). The respective scale factors are indicated.

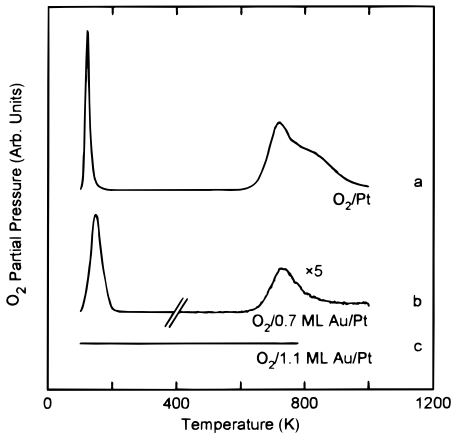

Figure 3. Desorption of a saturation coverage of oxygen from three gold coverages: (a) gold-free platinum, (b) 0.7 ML Au/Pt(335)—the region above 400 K has been expanded by a factor of 5, and (c) 1.1 ML Au/Pt(335). Curve (c) stops at 800 K because the Au is unstable above this temperature.

but does not eliminate, oxygen dissociation. Thermal desorption and low-energy electron diffraction (LEED) data suggest a surface on which bare Pt terraces coexist with Au-covered step sites and regions completely covered with Au. Oxygen does not adsorb on the gold-covered regions. CO does adsorb there, and it reacts with O on the Pt terraces below 200 K—lower than on bare Pt.

2. Experimental Section

The experiments took place at the General Motors Research and Development Center. The high-resolution electron energy loss spectroscopy (HREELS) system[37] was operated in the specular direction with 2 eV incident energy. Energy-loss resolution was 60 to 70 cm^{-1}. Temperature-programmed desorption (TPD) and reaction (TPR) data were collected by dosing the sample with combinations of CO and O_2 and ramping the temperature at 10 K/s to approximately 1000 K. The sample was placed 1 cm from the 0.5 cm diameter aperture of the mass spectrometer, which effectively eliminated signals from the back of the sample and from the supports.

Under some conditions exposure of the mass spectrometer to CO resulted in a spurious signal at mass 44. As a result, a small apparent yield of CO_2 was observed even in the absence of adsorbed oxygen. For the data presented here the spurious CO_2 signal was never more than a few percent of the maximum CO_2 yield.

The sample was cleaned by Ar ion sputtering and O_2 dosing while hot, as described elsewhere.[25] Gold was evaporated from a well-outgassed filament. The sample was heated to 500 K and then cooled to ~100 K before the shutter was opened to permit gold deposition. During deposition, the chamber pressure was $\sim 5 \times 10^{-10}$ Torr. A 1 h deposition gave ~1.1 ML Au. The Au was usually removed by Ar ion sputtering. Alternatively, flashing the sample to 1100−1150 K was sometimes used to reduce the gold coverage essentially to zero, probably by diffusion into the bulk.[38]

The gold coverage was determined by Auger spectroscopy, using the calibration established by Sachtler et al. for Au on Pt(111).[39,40] Figure 1 shows Auger spectra for clean Pt(335) and the two gold coverages studied in this work: approximately 0.7 and 1.1 ML gold. To clean the Au-coated sample, a parallel-array doser applied $\sim 10^{-8}$ Torr O_2 while the sample temperature was cycled repeatedly between 700 and 1000 K. Auger spectra after this treatment typically showed a barely detectable carbon peak—intensity ~0.3% of the platinum 69 eV transition for the 0.7 ML Au/Pt(335) surface shown in Figure 1b. After treatment, the surface's desorption and reaction properties were reproducible.

3. Adsorption of Oxygen and CO

3.1. Bare Pt(335). The adsorption of both CO and oxygen on Pt(335) has been well documented.[17,19,25,41−44] Thermal desorption spectra for saturation coverages of CO and oxygen are shown as curve (a) in Figure 2 and Figure 3, respectively. CO shows two desorption features: an edge-bonded species at 550 K and a terrace-bonded species at 400 K. These states fill sequentially. The edge sites are filled to saturation before population of the terrace begins.[17,41,43,44]

Oxygen desorption from Pt(335) shows three major features: molecular desorption from the terrace at 120 K, atomic recombination on the terrace at 750 K and atomic recombination from the steps at 850 K. A weak molecular desorption from the step site at 210 K has also been documented.[25]

3.2. Pt(335) with 1.1 ML Au. Curves (c) in Figures 2 and 3 shows the desorption of CO and oxygen, respectively, from the 1.1 ML Au/Pt(335) surface. Oxygen does not adsorb in either a molecular or atomic form on this surface from gas-phase O_2, at any temperature above 90 K. In this respect the fully Au-covered surface resembles gold single-crystal surfaces.[28−30]

The CO adsorption properties of the 1.1 ML Au/Pt(335) surface, however, differ from single-crystal gold. CO does not chemisorb on Au(111) and Au(110) down to temperatures of 100 and 125 K, respectively.[28,30] Deposited Au films adsorb CO above 110 K only when the Au has been deposited on a cold substrate.[45,46] We observe a single CO desorption feature at 105 K with two small shoulders at 190 and 220 K, as shown in Figure 2c. These adsorption states, not observed on single-crystal Au surfaces, may reflect the influence of the underlying Pt or arise from structural defects in the film. CO chemisorption on gold films deposited below room temperature has been attributed to atomic-scale defects.[45]

The desorption curves in Figures 2 and 3 show that the gold fully covers the Pt surface, since the desorption peaks characteristic of adsorption on Pt are completely eliminated. The Au-covered surface exhibited no LEED pattern, indicating both that the Pt is fully covered and that the Au is disordered.

3.3. Pt(335) with 0.7 ML Au. Our designation for the partially gold-covered Pt(335) surface is 0.7 ML Au/Pt(335). Auger measurements showed that it was covered with 0.6−0.8 ML Au.

We model the 0.7 ML Au/Pt surface as follows: the step edges are passivated with Au atoms almost everywhere, even on the Pt regions that are largely free of Au and are at least 30% of the surface. These coexist with completely Au-covered regions. This model is supported by LEED and TPD observations. It is consistent with previous observations of Au island formation on Pt(111)[38] and of Au/Pt segregation in ZrO_2-supported bimetal catalysts.[35] The LEED pattern of the 0.7 ML Au/Pt(335) surface was identical to that of the clean Pt(335) surface. In particular, the spots in the pattern had approximately the same size. Since the fully Au-covered surface is disordered, the diffraction pattern presumably comes from Pt regions that are largely free of Au. From TPD of oxygen and CO, we learn that even in these regions Au occupies the step sites.

Scanning tunneling micrographs of a sample with this Au coverage, taken in air, show three-dimensional gold islands with an average diameter of ∼300 nm and a height of two Au lattice spacings (0.7 nm). These micrographs indicate that the area of the surface that is platinum-like may be greater than the 30% indicated by Auger spectroscopy. There was insufficient resolution to determine the atomic-scale structure.

Oxygen Adsorption on 0.7 ML Au/Pt(335). Dissociation of oxygen on Pt(335) occurs almost exclusively at the step edges, and recombination of atomic oxygen at edge sites is characterized by a desorption peak near 850 K.[25] Figure 3b shows saturation oxygen desorption from 0.7 ML Au/Pt(335); the total amount of atomic oxygen (desorbing above 400 K) is only 10% of that on the clean Pt(335) surface, and the edge O peak near 850 K is missing. Evidently gold suppresses O_2 dissociation and eliminates oxygen adsorption at the step sites. There is no peak between 500 and 600 K, which would be characteristic of recombinative oxygen desorption from Au.[29]

It is interesting that atomic oxygen adsorption is reduced to 10% of its bare-surface value even though at least 30% of the Pt remains uncovered. Even extended exposures at 300 K do not produce a significantly higher oxygen coverage. We suggest that with the step sites passivated by gold, only a small number of dissociation sites remain. We further suggest that the dissociation sites on the 0.7 ML Au/Pt surface may be different from those that exist on bare Pt(335). Evidence for this is given in Section 4. Scanning tunneling microscope observations have shown that below 200 K dissociated oxygen atoms on Pt(111) move only a few lattice spacings before being frozen.[47] Other studies have shown that oxygen remains effectively immobile up to 450−500 K.[48] Once the adsorption sites near the dissociation sites are filled, further adsorption of atomic oxygen is prevented, even though open adsorption sites on Pt remain elsewhere on the surface.

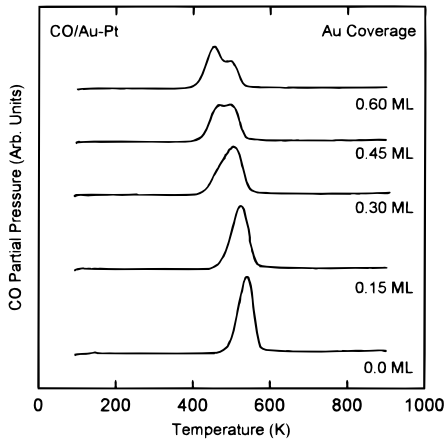

Figure 4. TPD of 0.07 ML of CO at five different coverages of gold on Pt(335). The change in desorption peak temperature is discussed in the text.

CO adsorption. Gold at step sites reduces and modifies CO adsorption, but does not eliminate it. For five gold coverages, Figure 4 shows the desorption of a small coverage of CO. [With 0.0 ML gold, the initial CO coverage was 0.07 ML, based on 0.69 ML CO at saturation on clean Pt(335).[44] An equal CO exposure was used to prepare for each of the TPD scans.] On the gold-free surface, only step sites are occupied at this CO coverage, as indicated by the desorption peak at 550 K. By 0.3 ML Au, a lower temperature shoulder indicates occupation of terrace sites and the step site peak has shifted down by 40 K. At 0.6 ML Au the predominant CO desorption feature is from the terrace sites, though a noticeable step peak remains, indicating that many of the step binding sites have been blocked by Au.

Figure 2b shows CO desorption from a saturated layer on 0.7 ML Au/Pt(335). The step site peak at 560 K is suppressed. Terrace desorption near 450 K is reduced. There are also three new desorption peaks below 300 K. The total amount of CO adsorbed is ∼55% of the saturation coverage on bare Pt(335) or approximately 0.4 ML.[44] The lowest temperature feature, at 120 K, is similar to that seen on the fully Au-covered surface, but the other two features, at 190 and 240 K, are specific to the partially Au-covered surface. We designate the desorption peaks below 300 K as "alloy" states.

Similar states have been seen[49] for Ru(0001) partially covered with Cu but not if the Ru is partially covered with Au. On Ru(0001), at low Au coverage, each Au atom blocks one CO adsorption site if the Au is deposited at 300 or 540 K, but not if the Au is deposited at 1110 K.[49,50] This has been attributed to Au island formation during low-temperature Au deposition and the possible formation of a surface alloy for Au deposited at 1110 K.

Isotope mixing experiments, shown in Figure 5, demonstrate that the CO desorption peaks correspond to distinct adsorption states. In each experiment the 0.7 ML Au/Pt(335) sample was saturated with $^{12}C^{16}O$ at 88 K, heated to the indicated temperature to remove selected desorption peaks, and then redosed to saturation with $^{12}C^{18}O$ at 88 K. The TPD spectra of the two isotopes were then measured simultaneously. In each case the first-dosed isotope appears only in the states that were not desorbed in the initial flash, and the later-dosed isotope only in

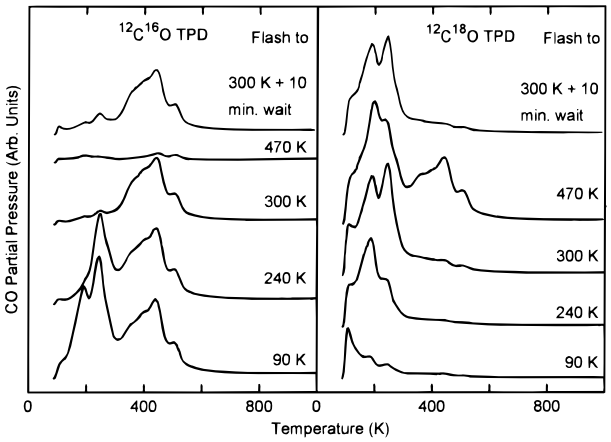

Figure 5. Isotopic mixing experiment with $^{12}C^{16}O$ and $^{12}C^{18}O$ on 0.7 ML Au/Pt(335). Details are given in the text. No appreciable mixing between the platinum and "alloy" states could be seen after selective dosing of $^{12}C^{16}O$ on platinum and $^{12}C^{18}O$ on the "alloy" sites.

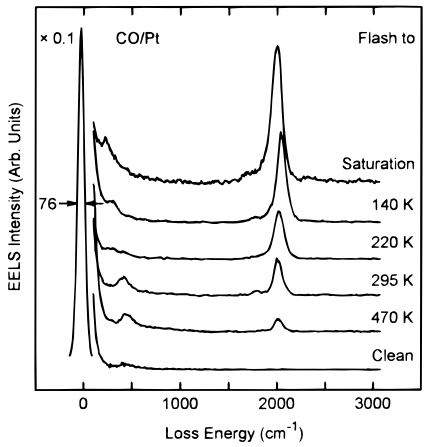

Figure 6. HREEL spectra of CO on 0.7 ML Au/Pt(335) at five coverages achieved by successive anneals. Peak positions and proportions are discussed in the text.

the states that were emptied by the flash. *Virtually no mixing of the isotopes is observed*, clearly indicating that each peak represents a distinct state, and that mixing of the CO between states does not occur on the time scale of a TPD.

The integrated intensity of the desorption from the "Pt" states (above 300 K) in Figure 2b is 30% of the desorption from the clean Pt(335) surface (Figure 2a), in proportion to the minimum fraction of Pt surface not covered by Au. Sachtler et al. have noted a similar linear decrease in CO desorption with gold coverage on a Au/Pt(553) surface.[40] The suppression of step desorption by Au was not as strong on that surface as we observe on the (335) surface, perhaps because the steps have a different orientation.

The HREEL spectrum for CO on this surface, shown in Figure 6, shows four features: the C═O stretch vibration of atop-bonded CO near 2100 cm^{-1}, the C═O stretch vibration of bridge-bonded CO near 1850 cm^{-1}, and two C-metal stretch modes at 350 and 475 cm^{-1}. (The frequencies of step CO and terrace CO are too close together to be resolved by HREELS.[10,19,41,43,44])

In the C═O stretch region the most interesting aspect is the weakness of the bridging peak at ∼1800 cm^{-1}, which on the bare Pt(335) surface can have more than 40% of the intensity of the atop peak.[41] The maximum bridge-to-atop intensity ratio in Figure 6 is 0.10, and occurs after a flash to 300 K has removed the CO bonded in "alloy" states. The intensity of the

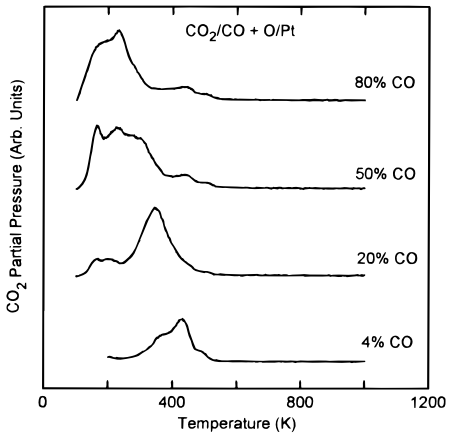

Figure 7. TPR of CO and oxygen on 0.7 ML Au/Pt(335). The surface was first prepared with adsorbed atomic oxygen at 20% of the saturation coverage. It was then dosed with CO to add the coverages listed. The surface used for 4% CO contained both O and O_2, the others were heated to 300 K before CO dosing so that only O was present.

atop peak decreases continuously with increasing annealing temperature, indicating that the peak includes unresolved contributions from both "alloy" and "Pt"-bonded CO. Atop CO on the Pt(335) terraces has a vibrational frequency[19,43,44] near 2100 cm^{-1}. Atop CO has a frequency between 2100 and 2125 cm^{-1} on evaporated Au,[45] and near 2110 cm^{-1} on supported Au particles.[34,35] It is therefore not surprising that the two species cannot be distinguished with our instrumental resolution (60−70 cm^{-1}) on these samples. We can conclude that the "alloy" states are exclusively atop-bonded.

The carbon−metal stretch of atop CO on Pt(111) is near 475 cm^{-1}, while that of bridge-bonded CO is near 380 cm^{-1} but about a factor of 6 weaker.[51−55] It is unlikely that the 350 cm^{-1} peak that we observe arises from bridge-bonded CO; it is more likely to be related to CO bonded on "alloy" sites. The low frequency of the peak and its disappearance when CO in the "alloy" states is desorbed are consistent with this identification. It is interesting that the 475 cm^{-1} peak is not seen until the 350 cm^{-1} peak disappears, even though both Pt and "alloy" states are occupied at saturation (as the TPD data in Figure 5 clearly show).

4. CO Oxidation

4.1. Temperature-Programmed Reaction. The most striking difference between the 0.7 ML Au/Pt(335) surface and the bare stepped Pt(335) and Pt(112) surfaces is the large CO_2 yield at low temperatures. Figures 7 and 8 show CO_2 production and CO desorption over 0.7 ML Au/Pt(335). The surface was prepared to have 20% of a saturation coverage of atomic oxygen by dosing with O_2 and then heating to 300 K to remove molecular oxygen. The surface was then dosed with CO to the coverage shown. [Coverages in this section are given relative to the maximum attainable on 0.7 ML Au/Pt(335).] No desorption of oxygen was detectable. Four major reaction peaks can be seen in Figure 7, at approximately 450, 350, 250, and 150 K. At low CO coverage (<20%), the reaction occurs predominantly above 300 K, and the curves resemble those for bare Pt(111), Pt(112), and Pt(335). At higher CO coverages the TPR curves are radically different from those seen on bare Pt, with virtually all of the CO_2 produced below room temperature. Significant low-temperature CO_2 production has been observed on bare Pt(112) and (335), but always less than half of the total yield.[18,19]

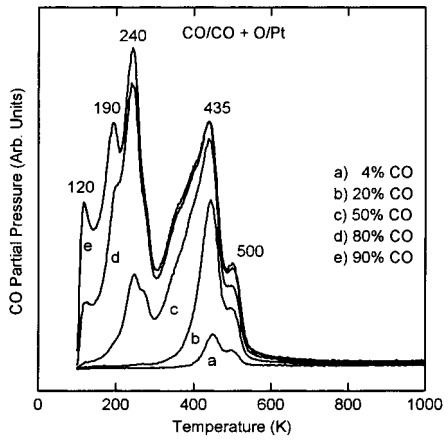

Figure 8. Desorption of CO during the reactions shown in Figure 7. CO desorption curves for other oxygen coverages were similar, as shown in Figure 9.

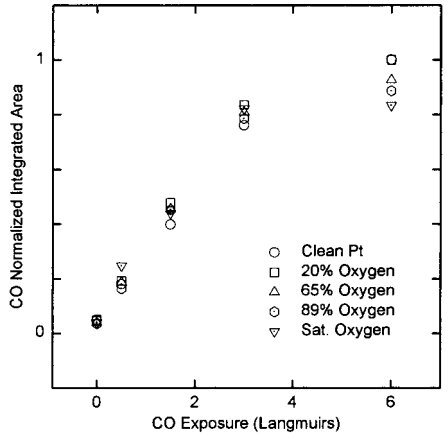

Figure 9. CO coverage on 0.7 ML Au/Pt(335) as a function of CO dosage, for five different oxygen coverages. The coverages are normalized to the saturation coverage with no oxygen. Very small amounts of CO are consumed during TPR.

The CO desorption traces in Figure 8 are virtually identical to those with no adsorbed oxygen or with the maximum achievable oxygen coverage. This point is emphasized in Figure 9, which shows the integrated CO desorption as a function of CO exposure for five different oxygen precoverages. Oxygen has a detectable effect only at the highest CO dose.

We make four observations. First, the reaction yield is limited by the amount of adsorbed oxygen. Since the 0.7 ML Au/Pt(335) surface can accommodate only 10% as much O as the gold-free surface, the amount of oxygen present in Figures 7 and 8 is only 2% of the original gold-free surface's saturation coverage—and essentially all of it reacts. This is demonstrated by the absence of O_2 desorption. Figure 10 shows the CO_2 yield as a function of the initial oxygen and CO coverages. The dependence on oxygen coverage is essentially linear, independent of CO coverage, indicating that the yield is limited by oxygen availability. For CO coverages greater than ~20%, the yield remains oxygen-limited up to the maximum achievable oxygen coverage. There is almost no dependence on CO coverage except at the very lowest CO coverages.

Second, CO in "alloy" states reacts at a lower temperature than CO on the Pt terraces, *even though the oxygen is bound on the Pt terrace sites*. This conclusion is supported by Figures 7 and 8. As the CO coverage is increased, CO_2 production below 300 K begins when the "alloy" states become occupied by CO. In addition, the reaction with "alloy" CO goes to completion before any reaction occurs with CO on Pt sites: CO_2 production

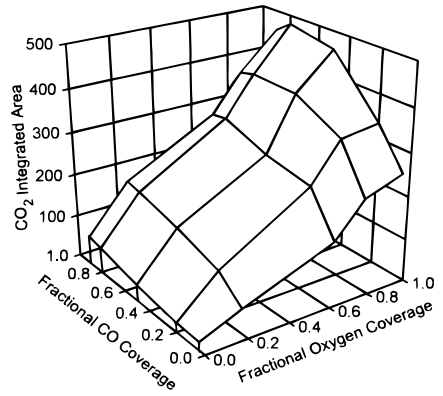

Figure 10. Integrated area under the CO_2 reaction curves as a function of CO and oxygen coverages. CO_2 production shows an approximately linear increase with O coverage, and an almost flat response with CO coverage, except at extremely low CO coverage, indicating a reaction that is limited by the availability of oxygen.

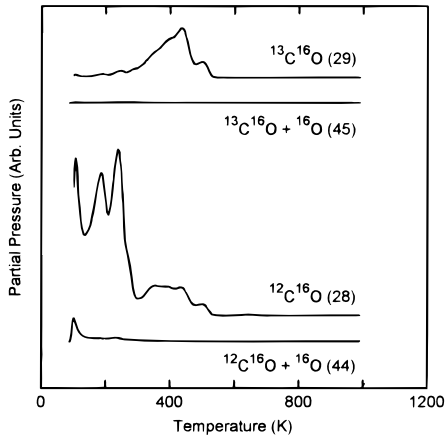

Figure 11. TPR with two CO isotopes. $^{13}C^{16}O$ was initially dosed and annealed to fill a majority of the Pt terrace sites, followed by a dose of both atomic and molecular oxygen, and then $^{12}C^{16}O$ to complete saturation. The absence of $^{13}C^{16}O_2$ indicates that the low-temperature reaction takes place between O adsorbed on the "alloy" states and oxygen on the platinum terraces.

above 300 K (from "Pt" sites) is observed only when there is no remaining CO on "alloy" sites, as indicated by the absence of CO desorption below 300 K.

The isotope mixing experiments shown in Figure 11 provide further confirmation of this sequence. The surface was first dosed at 90 K with enough $^{13}C^{16}O$ to fill most of the Pt terrace sites. This was followed by a long exposure to oxygen during which the sample temperature was raised to 300 K (to dissociate molecular oxygen) and then lowered to 90 K, giving a surface with the maximum coverage of both atomic and molecular oxygen achievable given the initial CO coverage. Finally, the sample was exposed to $^{12}C^{16}O$ at 90 K to saturate the "alloy" states. $^{12}CO_2$ production at mass 44 is then characteristic of reactions involving CO on the "alloy" states and $^{13}CO_2$ at mass 45 of reactions involving CO on the Pt terrace sites. Virtually all of the CO_2 is produced below 300 K and has mass 44, confirming that the low-temperature reaction channel involves CO on the "alloy" sites.

Third, the fact that the reaction with "alloy" site CO goes to completion before any reaction occurs with Pt-site CO implies that the oxygen must be bound in sites close to the boundaries between the bare and Au-covered regions of the surface. We assume that oxygen is immobile at least below 250 K.[47,48] If oxygen were bound in the middle of a bare Pt region, CO from the "alloy" states would have to diffuse across the terrace

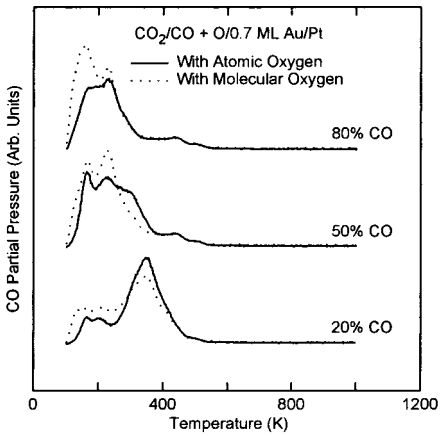

Figure 12. Comparison of CO_2 production under identical dosing conditions with and without adsorbed O_2. The surface with only atomic oxygen was prepared by annealing the surface to 300 K after the initial O_2 dose. Adsorbed O_2 enhances the lower-temperature reaction peaks, with the effect becoming more pronounced at high CO coverages.

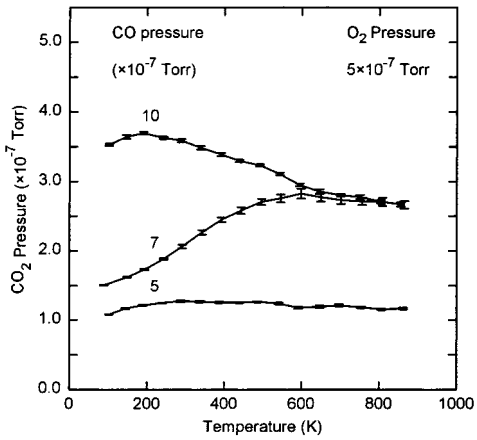

Figure 13. SSR measurement of CO oxidation in a constant oxygen background pressure of 5×10^{-7} Torr with the CO pressures listed. Note that increasing CO pressure does not inhibit CO_2 production, even at low temperature. Data shown by error bars with lines as guides for the eye.

(already saturated with CO) before reacting, and would have no higher probability of reacting than CO already on the bare Pt sites. We have already argued that oxygen dissociation occurs at a relatively small number of sites, and that the dissociated atoms move at most a few lattice spacings before becoming immobilized. The reaction data are consistent with that argument if the dissociation sites are near the boundaries between bare and Au-covered regions.

Fourth, because we see significant CO_2 production from thermally equilibrated O atoms and adsorbed CO at temperatures below 200 K, the activation barrier to the CO + O step in CO oxidation, though coverage dependent, can clearly be lower than on bare Pt, even for reaction with isolated atoms.

4.2. Reaction with Molecular Oxygen. The TPD traces in Figure 7 (except for 4% CO) were measured with only atomic oxygen on the surface. On Pt(111) a low-temperature reaction pathway has been observed only at high CO coverage and with molecular oxygen present.[8,11] Figure 12 shows that the same conditions on the 0.7 ML Au/Pt(335) surface also enhance CO_2 production below 300 K. Each pair of traces compares CO_2 production with the same initial oxygen and CO coverages. For the atomic oxygen traces the sample was flashed to 300 K after the oxygen dose but before dosing with CO. For the molecular oxygen experiment the CO was dosed at 90 K immediately after the oxygen dose.

4.3. Steady-State Reaction. We also measured the steady-state reaction of CO and oxygen on this sample starting at 100 K. The reaction kinetics below room temperature, while intriguing, may not directly reflect the behavior of Au/Pt electrodes on electrochemical sensors, which typically operate above 500 K. The carefully prepared coadsorbed layers used in the TPR measurements may also differ significantly from the surface coverages and distributions under steady-state reaction conditions. To investigate the steady-state reaction (SSR) behavior of the 0.7 ML Au/Pt(335) surface, the sample was placed in front of the mass spectrometer and the oxygen partial pressure was fixed at 5×10^{-7} Torr, while the temperature was varied from 100 to 900 K and the CO partial pressure P_{CO} was varied from 1×10^{-7} to 1×10^{-6} Torr. No appreciable CO_2 yield was observed for $P_{CO} \leq 5 \times 10^{-7}$ Torr. At each temperature and P_{CO}, the partial pressures in the chamber were allowed to stabilize and were then measured. The resulting curves of CO_2 partial pressure as a function of sample temperature are shown in Figure 13.

A possible complication in this technique is dissociation of oxygen by the mass spectrometer filament, a phenomenon used by Sault et al. to expose Au(100) to atomic hydrogen and oxygen.[55] It is possible that our results were affected by the resulting O dose, although the O_2 pressures we used were 10−100 times lower than in ref 55. If the O dose was significant, we would have expected to have produced CO_2 on a fully gold-covered surface. However, SSR measurements on the 1.1 ML Au/Pt(335) surface showed no significant production.

The behavior shown in Figure 13, particularly at low temperature, is quite different from that of gold-free Pt surfaces. On a gold-free surface, preadsorbed CO inhibits O adsorption, while preadsorbed O has little effect on CO adsorption. CO, however, desorbs at lower temperatures than oxygen.[3] Well below the CO desorption temperature, therefore, a high CO coverage builds up, which inhibits oxygen adsorption. The reaction rate is low, but increases exponentially with increasing temperature, with an activation energy essentially equal to the CO binding energy. The rate *decreases* with increasing P_{CO}. Somewhat above the CO desorption temperature, the surface becomes oxygen-covered and the reaction is limited by the CO arrival rate. The rate *decreases* gradually with increasing temperature, because of the reduced residence time of the CO, and increases with increasing P_{CO}. As a function of temperature, therefore, the reaction rate exhibits a maximum near the temperature at which the CO coverage falls to a small enough value that it does not strongly inhibit oxygen adsorption.[3,12,56,57]

On the 0.7 ML Au/Pt(335) surface we would expect similar behavior, though with lower overall reaction rates owing to the suppression of oxygen dissociation by the Au. In low-temperature TPD measurements, 30% of the saturation coverage of CO effectively prevents oxygen adsorption. At low temperature and high P_{CO}, therefore, the high CO coverage should inhibit oxygen adsorption, and the reaction rate should be low with an inverse (negative order) dependence on P_{CO}. Instead, the reaction rate at 100 K more than doubles when P_{CO} is increased from 7×10^{-7} to 1×10^{-6} Torr. Under the conditions we studied the reaction rate always increased with increasing P_{CO}.

Somewhat similar behavior has been observed in CO oxidation over Au particles on metal oxide surfaces. The increase in reaction rate with temperature is more gradual than on Pt,[31,32,36] and the reaction is positive-order in CO pressure.[33] In those cases the lack of inhibition is readily understood, since CO does not adsorb strongly either on the gold or on the oxide surface.

The present case is much more puzzling since the TPD results indicate a definite exclusion of oxygen by adsorbed CO. Even though the CO + O activation barrier is lower in this system, the complete absence of an inhibition effect is very surprising and is not fully understood.

Even at low temperature, then, the reaction is apparently limited by the CO pressure. The very strong dependence on P_{CO} at 100 K suggests that the reaction is dominated by the most weakly bound CO species, which desorbs even at 100 K and so has a P_{CO}-dependent coverage. For $P_{CO} \geq 7 \times 10^{-7}$ Torr, as the temperature increases further, the reaction rate becomes sufficient to reduce the oxygen coverage, causing a gradual transition into a regime where oxygen availability limits the reaction rate. For $P_{CO} = 5 \times 10^{-7}$ Torr the reaction rate reaches a maximum near 600 K and then gradually decreases at higher temperatures. It is possible to attribute the rolloff to the onset of oxygen desorption, as well as decreased CO residence time. For $P_{CO} = 10 \times 10^{-7}$ Torr, however, the peak occurs at 200 K, far below any oxygen desorption.

At the highest temperatures, $T > 700$ K, both oxygen and CO desorb and react rapidly, and their coverages are low. For $P_{CO} < 5 \times 10^{-7}$ Torr the reaction remains limited by the CO pressure. At higher P_{CO} the reaction rate becomes high enough that the oxygen coverage is reduced and the reaction becomes limited by the oxygen pressure, as reflected in the absence of a P_{CO}-dependence at high T and high P_{CO}.

The SSR behavior of this surface at low T and high P_{CO} is anomalous. Bare Pt surfaces exhibit virtually no CO oxidation at temperatures below 300 K, but the weakly bonded CO states on the Au-covered regions generate significant chemical activity even at 100 K. The lack of an inhibition effect of CO and the very low temperature of the reaction rate peak for $P_{CO} = 1 \times 10^{-6}$ Torr, however, are very puzzling. In this regime many different CO adsorption states are occupied and both molecular and atomic oxygen may be present on the surface, so the microscopic phenomena are no doubt complex. Further investigation will be needed to clarify the drastic changes in SSR behavior introduced by the partial Au overlayer.

5. Conclusions

A stepped Pt surface, partially covered with Au, exhibits new adsorptive and catalytic behavior different from those of either bare Pt or pure Au surfaces. These properties may help to explain the performance of exhaust gas sensors with Au/Pt alloy electrodes.

A partial coverage of Au strongly affects the dissociation and adsorption of oxygen on Pt(335). A fully Au-covered surface is inert to oxygen dissociation. On the gold-free Pt(335) surface, oxygen dissociation occurs almost exclusively at steps. With 0.7 ML of Au, the adsorption of oxygen at step sites is eliminated and the saturation oxygen coverage is reduced to only 10% of its value on the bare Pt surface—even though at least 30% of the surface remains uncovered by Au. The oxygen dissociation that remains is confined to sites near the Au−Pt boundaries. After dissociation, the oxygen atoms stay within a few lattice spacings of the Au−Pt boundaries.

The ability of Au/Pt electrodes to exhibit nonequilibrium behavior in sensor applications is qualitatively explained by gold's effect on oxygen adsorption—especially at high temperatures, where step sites are likely to dominate the kinetics. Surprisingly, however, 0.7 ML gold also makes it possible for CO and O to react at an even lower temperatures than on pure Pt. This is explained as mobile CO on the surface reacting with O near the Au−Pt boundaries to form CO_2 below 300 K—temperatures at which CO on the bare Pt surface only reacts at a significant rate with "hot" oxygen atoms.

The steady-state reaction behavior at low temperatures is quite different from that over bare Pt. An increase in CO partial pressure did not inhibit CO oxidation under any of the conditions studied. This suggests that adsorbed CO does not completely block all of the sites at which oxygen dissociates.

Acknowledgment. This work was supported in part by the National Science Foundation under Grants #DMR-9510267, DMR-9696233, and DMR-9400417 (MRSEC). It was also supported by the Center for Sensor Materials at Michigan State University. We thank Charles Olk and Baokang Bi for taking scanning tunneling and atomic force micrographs of the surface.

References and Notes

(1) Baier, G.; Schüle, V.; Vogel, A. *Appl. Phys. A* **1993**, *57*, 51.
(2) Vogel, A.; Baier, G.; Schüle, V. *Sensors and Actuators B* **1993**, *15*−*16*, 147.
(3) (a) Engel, T.; Ertl, G. *Adv. Catal.* **1979**, *28*, 1. (b) Engel, T.; Ertl, G. In *The Chemical Physics of Solid Surfaces and Heterogeneous Catalysis*; King, D. A., Woodruff, D. P., Eds.; Elsevier: Amsterdam, 1982; Vol. 4, pp 73−93.
(4) Shigeishi, R. A.; King, D. A. *Surf. Sci.* **1978**, *75*, L397.
(5) Nieuwenhuys, B. E. *Surf. Sci.* **1983**, *126*, 307.
(6) Gland, J. L.; Kollin, E. B. *J. Chem. Phys.* **1983**, *78*, 963.
(7) Gland, J. L.; Kollin, E. B. *Surf. Sci.* **1985**, *151*, 260.
(8) Matsushima, T. *Surf. Sci.* **1983**, *127*, 403.
(9) Akhter, S.; White, J. M. *Surf. Sci.* **1986**, *171*, 527.
(10) Szabó, A.; Kiskinova, M.; Yates, J. T., Jr. *J. Chem. Phys.* **1989**, *90*, 4604.
(11) Yoshinobu, J.; Kawai, M. *J. Chem. Phys.* **1995**, *103*, 3220.
(12) Coulston, G. W.; Haller, G. L. *J. Chem. Phys.* **1991**, *95*, 6932.
(13) Wei, C.; Haller, G. L. *J. Chem. Phys.* **1996**, *105*, 810.
(14) Mieher, W. D.; Ho, W. *J. Chem. Phys.* **1989**, *91*, 2755.
(15) Mieher, W. D.; Ho, W. *J. Chem. Phys.* **1993**, *99*, 9279.
(16) Yates, J. T., Jr. *J. Vac. Sci. Technol. A* **1995**, *13*, 1359.
(17) Xu, J.; Henriksen, P.; Yates, J. T., Jr. *J. Chem. Phys.* **1992**, *97*, 5250.
(18) Szabó, A.; Henderson, M. A.; Yates, J. T., Jr. *J. Chem. Phys.* **1992**, *96*, 6191.
(19) Xu, J.; Yates, J. T., Jr. *J. Chem. Phys.* **1993**, *99*, 725.
(20) Hopster, H.; Ibach, H.; Comsa, G. *J. Catal.* **1977**, *46*, 37.
(21) Zaera, F.; Liu, J.; Xu, M. *J. Chem. Phys.* **1997**, *106*, 4204.
(22) McCarthy, E.; Zahradnik, J.; Kuczynski, G. C.; Carberry, J. J. *J. Catal.* **1975**, *39*, 29.
(23) Herskowitz, M.; Holliday, R.; Cutlip, M. B.; Kenney, C. N. *J. Catal.* **1982**, *74*, 408.
(24) Oh, S. H.; Fisher, G. B.; Carpenter, J. E.; Goodman, D. W. *J. Catal.* **1986**, *100*, 360.
(25) Wang, H.; Tobin, R. G.; Lambert, D. K.; DiMaggio, C. L.; Fisher, G. B. *Surf. Sci.* **1997**, *372*, 267.
(26) Yamanaka, T.; Matsushima, T.; Tanaka, S.-I.; Kamada, M. *Surf. Sci.* **1996**, *349*, 119.
(27) Matsushima, T. *Surf. Sci.* **1985**, *157*, 297.
(28) Outka, D. A.; Madix, R. J. *Surf. Sci.* **1987**, *179*, 351.
(29) Canning, N. D. S.; Outka, D.; Madix, R. J. *Surf. Sci.* **1984**, *141*, 240.
(30) Holmes Parker, D.; Koel, B. E. *J. Vac. Sci. Technol. A.* **1990**, *8*, 2585.
(31) Haruta, M.; Yamada, N.; Kobayashi, T.; Iijima, S. *J. Catal.* **1989**, *115*, 301.
(32) Kobayashi, T.; Haruta, M.; Tsubota, S.; Sano, H.; Delmon, B. *Sens. Act. B* **1990**, *1*, 222.
(33) Lin, S. D.; Bollinger, M.; Vannice, M. A. *Catal. Lett.* **1993**, *17*, 245.
(34) Boccuzzi, F.; Chiorino, A.; Tsubota, S.; Haruta, M. *Sens. Act. B* **1995**, *24*−*25*, 540.
(35) Boccuzzi, F.; Guglielminotti, E.; Pinna, F.; Strukul, G. *Surf. Sci.* **1997**, *377*−*379*, 728.
(36) Fukushima, K.; Takaoka, G. H.; Matsuo, J.; Yamada, I. *Jpn. J. Appl. Phys.* **1997**, *36*, 813.
(37) Sexton, B. A. *J. Vac. Sci. Technol.* **1979**, *16*, 1033.
(38) Davies, P. W.; Quinlan, M. A.; Somorjai, G. A. *Surf. Sci.* **1982**, *121*, 290.
(39) Sachtler, J. W. A.; Van Hove, M. A.; Bibérian, J. P.; Somorjai, G. A. *Surf. Sci.* **1981**, *110*, 19.
(40) Sachtler, J. W. A.; Somorjai, G. A. *J. Catal.* **1983**, *81*, 77.

(41) Luo, J. S.; Tobin, R. G.; Lambert, D. K.; Fisher, G. B.; DiMaggio, C. L. *Surf. Sci.* **1992**, *274*, 53.
(42) Rar, A.; Matsushima, T. *Surf. Sci.* **1994**, *318*, 89.
(43) Hayden, B. E.; Kretzschmar, K.; Bradshaw, A. M.; Greenler, R. G. *Surf. Sci.* **1985**, *149*, 394.
(44) Lambert, D. K.; Tobin, R. G. *Surf. Sci.* **1990**, *232*, 149.
(45) Dumas, P.; Tobin, R. G.; Richards, P. L. *Surf. Sci.* **1986**, *171*, 579.
(46) Stephan, J. J.; Ponec, V. *J. Catal.* **1976**, *42*, 1.
(47) Wintterlin, J.; Schuster, R.; Ertl, G. *Phys. Rev. Lett.* **1996**, *77*, 123.
(48) Lewis, R.; Gomer, R. *Surf. Sci.* **1968**, *12*, 157.
(49) Harendt, C.; Christmann, K.; Hirschwald, W.; Vickerman, J. C. *Surf. Sci.* **1986**, *165*, 413.
(50) Park, C. *Surf. Sci.* **1988**, *203*, 395.
(51) Tobin, R. G.; Richards, P. L. *Surf. Sci.* **1987**, *179*, 387.
(52) Malik, I. J.; Trenary, M. *Surf. Sci.* **1989**, *214*, L237.
(53) Ryberg, R. *J. Electron Spectrosc. Relat. Phenom.* **1990**, *54/55*, 65.
(54) Engström, U.; Ryberg, R. *Phys. Rev. Lett.* **1997**, *78*, 1944.
(55) Sault, A. G.; Madix, R. J.; Campbell, C. T. *Surf. Sci.* **1986**, ***169***, 347.
(56) Schwartz, S. B.; Schmidt, L. D.; Fisher, G. B. *J. Phys. Chem.* **1986**, *90*, 6194.
(57) Peden, C. H. F.; Goodman, D. W.; Blair, D. S.; Berlowitz, P. J.; Fisher, G. B.; Oh, S. H. *J. Phys. Chem.* **1988**, *92*, 1563.